

DR. MARCUS GUTJAHR (Orcid ID : 0000-0003-2556-2619)

DR. ED HATHORNE (Orcid ID : 0000-0002-7813-2455)

DR. JOE STEWART (Orcid ID : 0000-0003-3092-5058)

Article type : Original Article

Sub-Permil Interlaboratory Consistency for Solution-Based Boron Isotope Analyses on Marine Carbonates

Marcus **Gutjahr** (1)*, Louise **Bordier** (2), Eric **Douville** (2), Jesse **Farmer** (3, 4), Gavin L. **Foster** (5), Ed C. **Hathorne** (1), Bärbel **Hönisch** (3), Damien **Lemarchand** (6), Pascale **Louvat** (7), Malcolm **McCulloch** (8), Johanna **Noireaux** (7), Nicola **Pallavicini** (9), James W.B. **Rae** (10, 11), Ilia **Rodushkin** (9, 12), Philippe **Roux** (6, 13), Joseph A. **Stewart** (5, 14), François **Thil** (2) and Chen-Feng **You** (15)

(1) GEOMAR Helmholtz Centre for Ocean Research Kiel, Wischhofstrasse 1-3, 24148 Kiel, Germany

(2) Laboratoire des Sciences du Climat et de l'Environnement, LSCE/IPSL, CEA-CNRS-UVSQ, Université Paris-Saclay, F-91191 Gif-sur-Yvette, France

(3) Department of Earth and Environmental Sciences and Lamont-Doherty Earth Observatory of Columbia University 61 Route 9W Palisades, NY 10964, USA

(4) now at: Princeton University, Department of Geosciences, Guyot Hall, Princeton, NJ 08544 USA

(5) School of Ocean and Earth Science, University of Southampton, National Oceanography Centre, Southampton, European Way, Southampton SO14 3ZH, UK

(6) Laboratoire d'Hydrologie et de Géochimie de Strasbourg, EOST, Université de Strasbourg et CNRS, 1 rue Blessig, 67084 Strasbourg, France

(7) Institut de Physique du Globe de Paris, Sorbonne Paris Cité, Université Paris-Diderot, UMR CNRS 7154, 1 rue Jussieu, 75238 Paris Cedex 05, France

(8) ARC Centre of Excellence for Coral Reef Studies and School of Earth and Environment, The University of Western Australia, Crawley 6009, Australia

(9) ALS Scandinavia AB, Aurorum 10, SE-97775 Luleå, Sweden

(10) Geological and Planetary Sciences, Caltech, 1200 E California Blvd, Pasadena, California, 91125, USA

(11) School of Earth and Environmental Sciences, University of St Andrews, North Street, St Andrews, UK

(12) Division of Geosciences, Luleå University of Technology, S-971 87 Luleå, Sweden

This article has been accepted for publication and undergone full peer review but has not been through the copyediting, typesetting, pagination and proofreading process, which may lead to differences between this version and the [Version of Record](#). Please cite this article as [doi: 10.1111/GGR.12364](https://doi.org/10.1111/GGR.12364)

This article is protected by copyright. All rights reserved

(13) Biogéochimie des Ecosystèmes Forestiers, INRA, 54280 Champenoux, France

(14) School of Earth Sciences, University of Bristol, Queens Road, Bristol, BS8 1RJ, UK

(15) Isotope Geochemistry Laboratory, Department of Earth Sciences, National Cheng Kung University, No 1 University Road, 701 Tainan, Taiwan

* Corresponding author. e-mail: mgutjahr@geomar.de

Abstract

Boron isotopes in marine carbonates are increasingly used to reconstruct seawater pH and atmospheric pCO₂ through Earth's history. While isotope ratio measurements from individual laboratories are often of high quality, it is important that records generated in different laboratories can equally be compared. Within this Boron Isotope Intercomparison Project (BIIP), we characterised the boron isotopic composition (commonly expressed in $\delta^{11}\text{B}$) of two marine carbonates: Geological Survey of Japan carbonate reference materials JCp-1 (coral *Porites*) and JCt-1 (giant clam *Tridacna gigas*). Our study has three foci: (i) to assess the extent to which oxidative pre-treatment, aimed at removing organic material from carbonate, can influence the resulting $\delta^{11}\text{B}$; (ii) to determine to what degree the chosen analytical approach may affect the resultant $\delta^{11}\text{B}$, and (iii) to provide well-constrained consensus $\delta^{11}\text{B}$ values for JCp-1 and JCt-1. The resultant robust mean and associated robust standard deviation (s^*) for un-oxidised JCp-1 is $24.36 \pm 0.45\text{‰}$ ($2s^*$), compared with $24.25 \pm 0.22\text{‰}$ ($2s^*$) for the same oxidised material. For un-oxidised JCt-1, respective compositions are $16.39 \pm 0.60\text{‰}$ ($2s^*$; un-oxidised) and $16.24 \pm 0.38\text{‰}$ ($2s^*$; oxidised). The consistency between laboratories is generally better if carbonate powders were oxidatively cleaned prior to purification and measurement.

Keywords: mass spectrometry, Geological Survey of Japan, boron isotopes, carbonate reference materials, interlaboratory experiment.

Received 09 Jun 20 – Accepted 22 Sep 20

The boron isotope system is a non-traditional light stable isotope system with only two isotopes, ^{10}B and ^{11}B . The boron isotope ratio of any substrate is usually presented relative to an isotope reference material distributed by the National Institute of Standards and Technology in delta notation:

$$\delta^{11}\text{B}_{\text{NIST SRM 951}} = \frac{{}^{11}\text{B}/{}^{10}\text{B}_{\text{sample}}}{{}^{11}\text{B}/{}^{10}\text{B}_{\text{NIST SRM 951}}} - 1 \quad (1)$$

where NIST SRM 951 (or NIST SRM 951a) represents a boric acid isotopic reference material powder. NIST SRM 951 and NIST SRM 951a are essentially isotopically identical with a certified $^{10}\text{B}/^{11}\text{B}$ of 0.2473 ± 0.0002 . In recent decades, boron isotope ratios measured in biogenic carbonates have emerged as a valuable tool to determine past seawater pH, a key variable to reconstruct atmospheric CO_2 concentrations and other marine carbonate system parameters (Vengosh *et al.* 1991, Hemming and Hanson 1992). Boron isotope ratios in marine carbonates can be used as a pH indicator because of several key characteristics. First, boron behaves conservatively in seawater with a residence time of ~ 14 Ma (Lemarchand *et al.* 2000) and a resultant homogenous bulk seawater $\delta^{11}\text{B}$ of $39.61 \pm 0.04\text{‰}$ (Foster *et al.* 2010). Boron in seawater occurs as two aqueous species, boric acid ($\text{B}(\text{OH})_3$) and borate ion ($\text{B}(\text{OH})_4^-$) (Dickson 1990). The relative abundance of each species is pH-dependant (Vengosh *et al.* 1991, Hemming and Hanson 1992), resulting in the increasing proportion of borate ion under increasing pH conditions. Importantly, the $\delta^{11}\text{B}$ of borate ion is isotopically depleted compared with boric acid as a function of equilibrium isotope fractionation between the two species (Zeebe 2005, Klochko *et al.* 2006). The ratio of borate ion to boric acid increases significantly in the pH range of modern and palaeo-seawater (*ca.* 7.7 to 8.3 on the total pH scale). Since most marine calcifiers only incorporate borate ion into biogenic carbonates, it follows that their boron isotopic ratio provides direct information on ambient seawater (Vengosh *et al.* 1991, Hemming and Hanson 1992) or internal calcifying fluid pH (Rollion-Bard *et al.* 2003, Allison *et al.* 2010, McCulloch *et al.* 2012). While commonly applied to foraminifera (Hönisch and Hemming 2005, Foster 2008, Rae *et al.* 2011), in recent years the pH sensitivity of the boron isotope system has been explored in a variety of marine biogenic carbonates, including brachiopods (Lecuyer *et al.* 2002, Penman *et al.* 2013, Jurikova *et al.* 2019), corals (Hönisch *et al.* 2004, Reynaud *et al.* 2004, Wall *et al.* 2016, Cornwall

et al. 2017, Wu *et al.* 2018), molluscs (Heinemann *et al.* 2012) and coralline algae (Cornwall *et al.* 2017, Donald *et al.* 2017, Anagnostou *et al.* 2019).

The first investigations into the pH-dependent fractionation of $^{11}\text{B}/^{10}\text{B}$ during incorporation into CaCO_3 were published in the late 1980s (e.g., Balz *et al.* 1986, Oi *et al.* 1991). However, for many years significant offsets between individual laboratories (on the order of 2 to 11‰) permitted only limited comparability of $\delta^{11}\text{B}$ data between institutions (e.g., Aggarwal *et al.* 2009). This disagreement is not surprising since boron is a contamination-prone light stable isotope system that requires clean reagents and careful sample handling during purification and analysis, as well as a boron-free air handling system (e.g., Rosner *et al.* 2005). The latest study comparing the reproducibility condition of measurement of boron isotopic data reported good agreement for solutions of dilute boric acids and seawater samples, yet also revealed elevated interlaboratory isotopic offsets for identical carbonate sample materials on the order of up to $\sim 1.5\text{‰}$ ($2s$) (Foster *et al.* 2013). Only four laboratories participated in that study, and since then considerably more research groups have begun publishing carbonate-derived boron isotope data. For this reason, we present a timely update on the interlaboratory comparability of boron isotope data in commonly used marine carbonate reference materials.

Besides comparing different sample handling and mass spectrometric approaches, a further sample preparation step in the measurement procedure was tested within the frame of BIIP. We assessed the impact of oxidative cleaning techniques on biogenic carbonates, such as those frequently performed for other geochemical analyses (Boyle 1981, Barker *et al.* 2003). We present boron isotope results generated in ten individual laboratories, which reveal an unprecedented level of consistency of carbonate $\delta^{11}\text{B}$ results between laboratories. Given the comparison of cleaned and uncleaned material, we also identify potential pitfalls during the processing of carbonate samples for boron isotopic approaches that potentially compromise the high level of analytical agreement that is emerging between laboratories.

Materials

Two powdered and homogenised biogenic carbonates originally produced by the Geological Survey of Japan were analysed in ten different laboratories for our boron isotope interlaboratory comparison study (Table 1). The first carbonate used is JCp-1, a modern *Porites* sp. coral colony sampled 2 metres below mean sea level on the northeast coast of Ishigaki Island, Ryukyu Islands, Japan (24°33'N, 124°20'E). JCp-1 is entirely aragonitic and all surfaces of the corals in contact with the biological tissue were removed prior to processing (Okai *et al.* 2002). As outlined in the original publication, crushed coral material was washed with deionised water and dried prior to further grinding and homogenisation. The grain size fraction < 250 μm of JCp-1 material was sieved and distributed by the Geological Survey of Japan.

The second reference material used was also prepared by the Geological Survey of Japan (Inoue *et al.* 2004). Reference material JCt-1 is derived from a fossil mid-Holocene giant clam *Tridacna gigas* sampled near Kume Island, Japan (26°N, 126°E) in the central Ryuku Islands, Japan. It is also entirely aragonitic. Further details on powder preparation of JCt-1 were not provided in Inoue *et al.* (2004).

None of the powders were bleached prior to packing (Hathorne *et al.* 2013). Previously published trace elemental ratios presented by Hathorne *et al.* (2013) are reported for comparison in Table 1. Notably, Sr, Mg, Ba, B and Li have higher ratios relative to Ca in JCp-1, while JCp-1 has approximately fifty times higher U/Ca than JCt-1. At 460 $\mu\text{mol mol}^{-1}$, the molar B/Ca ratio in JCp-1 is ~ 2.4 higher than in JCt-1 which has 191 $\mu\text{mol mol}^{-1}$ (Hathorne *et al.* 2013).

Due to changes in CITES regulations (i.e., *Convention on International Trade in Endangered Species of Wild Fauna and Flora*; www.cites.org), neither of these biogenic carbonate materials are currently available for international distribution by the Geological Survey of Japan, but they remain common reference materials in many laboratories (e.g., Farmer *et al.* 2016, Lazareth *et al.* 2016, Raddatz *et al.* 2016, Stewart *et al.* 2016, Jurikova *et al.* 2019). Efforts are on-going to find suitable replacements and two isotope standard solutions artificially produced with carbonate matrices (NIST RM 8301 (Coral) and NIST RM 8301 (Foram)) will soon become available as consistency reference materials for boron isotopic and trace metal isotope studies (Stewart *et al.* in press).

Analytical and mass spectrometric approaches

Nine out of the ten laboratories participating in this study used an MC-ICP-MS-based approach to determine the $\delta^{11}\text{B}$ of the JCp-1 and JCT-1 reference materials; one used N-TIMS. With the exception of the N-TIMS approach, for which boron was not separated from the aragonitic matrix, elemental purification was carried out in all laboratories (Table 2). In eight laboratories, boron was purified using Amberlite™ IRA743 exchange resin on microcolumns (Gonfiantini *et al.* 2003, Foster 2008, Aggarwal *et al.* 2009, Paris *et al.* 2010, Louvat *et al.* 2011, Rae *et al.* 2011, Voinot *et al.* 2013, McCulloch *et al.* 2014, Roux *et al.* 2015) or using a batch method (Douville *et al.* 2010, Wu *et al.* 2018), and one laboratory employed the sublimation technique for boron purification (Wang *et al.* 2010). The boron total procedural blank ranged from below 8 pg to about 3000 pg between laboratories (Table 2). Sample ionisation during N-TIMS spectrometric measurement is achieved via heating of Re-metal filaments in a high-vacuum source chamber. For the MC-ICP-MS approaches, sample introduction was achieved using either: (i) a quartz spray chamber (Gonfiantini *et al.* 2003, Aggarwal *et al.* 2009, Douville *et al.* 2010, Wang *et al.* 2010, Voinot *et al.* 2013, McCulloch *et al.* 2014), (ii) a PFA spray chamber (Foster 2008, Rae *et al.* 2011), or (iii) direct injection (d-DIHEN) (Paris *et al.* 2010, Louvat *et al.* 2011, Louvat *et al.* 2014). Some of the laboratories used ammonia introduced via a second gas inlet into the spray chamber as an additional gas to aid washout between individual measurements (e.g., Foster 2008). None of the laboratories in this study used hydrofluoric acid to aid boron washout, although recent studies have shown this to be an effective alternative to an ammonia add gas (Misra *et al.* 2014, Rae *et al.* 2018). All laboratories used an (isotope-) calibrator-sample bracketing technique to derive $\delta^{11}\text{B}$. Except for the MC-ICP-MS method with direct injection as introduction system, on peak zeros were subtracted from respective ion beams in all MC-ICP-MS based approaches. This approach is necessary because of the typically poor washout of boron compared with other isotope systems and the relatively small signal sizes, requiring tight control over memory effects during sample introduction.

BIIP interlaboratory comparison routine protocol

In contrast to an earlier interlaboratory comparison study (Gonfiantini *et al.* 2003), participating laboratories were required to have a demonstrable record of producing $\delta^{11}\text{B}$ high-quality data. Every participating laboratory was sent 2 g of powder of each of the two reference materials. A minimum of six test portions of each reference material, weighing at least 5 mg each, were analysed in each laboratory. Three of these test portions were processed without any oxidative cleaning, and the other three underwent oxidative cleaning using either NaClO or H_2O_2 in dilute NH_4OH (Table 2). Each laboratory reported 2–10 results for each test portion digest, either as individual filament analyses (e.g., N-TIMS) or simply as repeat measurements of the same powder preparation (e.g., MC-ICP-MS). The key aim of our study was to assess consistencies and potential discrepancies between techniques with particular focus on analytical problems that could be improved in future studies. Therefore, the reported $\delta^{11}\text{B}$ data were compiled and statistically analysed by the first author, while the origin of each data set was kept anonymous as much as feasible.

Statistical data treatment

First, the average $\delta^{11}\text{B}$ value of each laboratory for the four individual sample sets (presenting either previously oxidised or un-oxidised JCp-1 or JCt-1 boron isotope results) was determined. This provides a total of ten independent laboratory mean $\delta^{11}\text{B}$ values for un-oxidised JCp-1 and nine mean $\delta^{11}\text{B}$ values for oxidised JCp-1 (Table 3). For JCt-1 reference material powders, nine $\delta^{11}\text{B}$ means from both un-oxidised and oxidised powders were reported (Table 4). Subsequently, the robust mean and associated robust standard deviation were calculated for each of the four data sets. To do so, we followed the ISO 13528:2015 data treatment procedure for normally distributed data sets as outlined in *approach 2* of Srnková and Zbiral (2009). The procedure of deriving the robust mean and robust standard deviation is iterative and the statistical analysis is repeated until no change in the calculated robust mean X^* and its robust standard deviation s^* is observed. The approach is outlined below.

An initial robust average X^* is calculated from the median of each laboratory's mean $\delta^{11}\text{B}$ (hence n being either 9 or 10). The associated initial robust standard deviation (representing the Median

Absolute Deviation, MAD) s^* is derived by multiplying the median of all laboratories' offsets from X^* from the interlaboratory median by 1.483. Calculation of $s^* = 1.483 \times MAD$ is a robust scaling factor applied in statistic applications for normally distributed data sets following the argument that the median absolute deviation covers 50% (between $\frac{1}{4}$ and $\frac{3}{4}$) of the standard normal cumulative distribution function (see 13528:2015(E) 2015). Next, a δ value is calculated via multiplication of the initial robust standard deviation with a factor 1.5. Then, $(X^* - \delta)$ as well as $(X^* + \delta)$ are calculated. If any laboratory's mean $\delta^{11}\text{B}$ falls below $(X^* - \delta)$, the actual laboratory mean $\delta^{11}\text{B}$ is replaced with $(X^* - \delta)$. If any laboratory's $\delta^{11}\text{B}$ mean falls above $(X^* + \delta)$, the actual laboratory mean $\delta^{11}\text{B}$ is replaced with $(X^* + \delta)$. Laboratory mean $\delta^{11}\text{B}$ values larger than $(X^* - \delta)$ and smaller than $(X^* + \delta)$ are kept, representing the vast majority of $\delta^{11}\text{B}$ values presented here. This exercise led to exclusion of the following mean $\delta^{11}\text{B}$ values: un-oxidised JCp-1 powders from laboratories 1 and 4 (laboratory numbers refer to corresponding numbers shown in Figures 1 and 2), un-oxidised JCT-1 powders from laboratories 1, 4 and 10, oxidised JCp-1 powders from laboratories 1 and 6, and oxidised JCT-1 powders from laboratories 6 and 10. For all four data sets (i.e., un-oxidised and oxidised JCp-1 and JCT-1), an updated X^* and s^* was then calculated and the above screening procedure repeated, resulting in no further exclusion of data. The resultant robust means and robust standard deviations discussed in the text and shown in Table 5, as well as in Figures 1 to 4 have been derived in this manner. We reiterate that the robust standard deviation is calculated using only the mean $\delta^{11}\text{B}$ per laboratory for each of the four data sets. As a measure of the integrity of reported average $\delta^{11}\text{B}$ from each laboratory we used a z-score:

$$z = (x_i - X^*) / s^* \quad (2)$$

in which x_i represents the individual laboratory average $\delta^{11}\text{B}$, X^* the robust mean, and s^* the robust standard deviation. An absolute z-score below or equal to 2 is considered to be acceptable, absolute z-score values between 2 and 3 are of likely questionable quality, or in the case of laboratory 10 reflect on a carbonate specific constant offset between N-TIMS and MC-ICP-MS (see also Foster *et al.* 2013). A z-score value beyond 3 suggests that results are outside the satisfactory range. Given that s^* is used for determining the z-score for each laboratory mean, this approach may systematically exclude certain laboratory results as outliers (i.e. those with most distinct $\delta^{11}\text{B}$ relative to X^*). However, given the distribution of our data sets, those mean

laboratory $\delta^{11}\text{B}$ that fell beyond a z -score of 3 are relatively clear cases of questionable quality (Figures 1, 2).

Results

Throughout Figures 1 to 3, the order of laboratories is kept the same in the respective panels, chosen so that Figure 1a displays $\delta^{11}\text{B}$ in increasing order, hence does not simply follow the order of laboratories shown in Tables 3 and 4. Range bars plotted in Figures 1a, b and 2a, b represent the reproducibility precision expressed as $2s$ of the three replicate analyses carried out in each laboratory. While a $2s$ derived from a population of three data points cannot provide an accurate 95% confidence limit, it becomes apparent from the individual reported $\delta^{11}\text{B}$ that range bars shown in this manner provide a reasonable insight into the intermediate precision of each laboratory (see Figures 1, 2 and Tables 3, 4). Range bars in Figure 3 display the provided $2s$ intermediate precision for each individually measured aliquot, which take into account the variable number of replications performed in each laboratory ($n = 2\text{--}10$, see Tables 3 and 4). The calculated robust means are shown as grey lines and the robust standard deviations $2s^*$ plotted as a shaded area in Figures 1a, b and 2a, b. The calculated z -score for each data point is shown in panels c and d. Laboratory means plotting within a z -score of -2 to 2 plot within the shaded area in panels of Figures 1c, d and 2c, d. The z -score threshold with an absolute value of 3 is marked with a dotted line on Figures 1 and 2.

We note that the few obvious outliers (identified via $|z| > 3$) in our interlaboratory comparison were all shifted towards lower reported $\delta^{11}\text{B}$ (Figures 1 and 2). Laboratory 4 only reported $\delta^{11}\text{B}$ for un-oxidised JCp-1 and JCt-1 reference material powders, and submitted ratios fall outside the z -score reliability threshold. Laboratory 6 provided results for oxidised standard $\delta^{11}\text{B}$ for both JCp-1 and JCt-1 that also fail this data screening criterion. Although $\delta^{11}\text{B}$ from Laboratory 6 for oxidised reference materials can be flagged as outliers, the un-oxidised mean $\delta^{11}\text{B}$ for both reference materials of Laboratory 6 agree well within the range of $\delta^{11}\text{B}$ reported from the majority of other laboratories.

The various mass spectrometry approaches (i.e., N-TIMS vs. ICP-MS) did not lead to any clear isotopic shift between reported $\delta^{11}\text{B}$ for JCp-1 yet potentially slightly higher $\delta^{11}\text{B}$ for JCt-1 for N-TIMS (Figures 1–3, Tables 3 and 4) (cf. Farmer *et al.* 2016). The choice of sample introduction system (i.e., quartz vs. PFA spray chamber, or alternatively direct injection) and purification method for the nine MC-ICP-MS based data sets also did not lead to resolvable differences in results (Figure 3). The results after ion exchange purification or using the sublimation technique both led to $\delta^{11}\text{B}$ with *z*-scores close to zero (not shown). Some laboratories reported elevated boron blank levels, however, these did not result in clearly distinct final $\delta^{11}\text{B}$ values (not shown).

Overall, the resultant robust mean and associated robust standard deviation for un-oxidised JCp-1 is $24.36 \pm 0.45\text{‰}$ ($2s^*$), compared with $24.25 \pm 0.22\text{‰}$ ($2s^*$) for the same material subjected to oxidative cleaning (Figure 4). For un-oxidised JCt-1, respective compositions are $16.39 \pm 0.60\text{‰}$ ($2s^*$) and $16.24 \pm 0.38\text{‰}$ ($2s^*$) for oxidised material. Hence, the robust means of cleaned and uncleaned powders are within error (for both reference material powders), but with the oxidised results only marginally lower than the un-oxidised material. A two-sided Student's *t*-test comparing laboratory means screened for outliers during the robust mean and robust standard deviation assessment; see methods above) provides a *p*-value of 0.12 for comparison of oxidised and un-oxidised JCp-1, and 0.17 for comparison of oxidised and un-oxidised JCt-1, confirming the populations are not different at 95% level of confidence. The difference in the mean values for the two reference materials in the respective laboratories (i.e., $\Delta\delta^{11}\text{B} = \text{mean } \delta^{11}\text{B}_{(\text{JCp-1})} - \text{mean } \delta^{11}\text{B}_{(\text{JCt-1})}$) is 7.98‰ for un-oxidised and 8.01‰ for oxidised reference materials. This difference in reference material $\delta^{11}\text{B}$ caused by cleaning is hence identical (within measurement precision) and suggests lack of preferential ^{11}B or ^{10}B removal for both reference materials.

In order to set the above reported robust means and robust standard deviations for JCp-1 and JCt-1 in context with alternative data handling approaches, we also report the results of two simpler statistical approaches: In the first alternative, we calculated the median of each data set ($n = 4$) using the respective individual mean of the $\delta^{11}\text{B}$ results of individual laboratories for each approach (un-oxidised or oxidised) and material (JCp-1 or JCt-1) ($n = 9$ or 10). While the resultant median for each data set is either very close or even identical to the robust mean, the resultant mean average deviation (not to be mistaken with the median average deviation, MAD) is

significantly smaller than our calculated robust standard deviation $2s^*$. The effect is most drastic for un-oxidised JCt-1 (Table 5). Repeating this exercise in a second alternative data treatment approach, now considering every replicate result for each of the four data sets again ($n = 27$ or 30) provides comparable median $\delta^{11}\text{B}$ values and slightly more expanded mean average deviations. Given that these mean average deviations are very close to or below the reported intermediate precision ($2s$) of individual laboratory results (see Tables 2 and 3), these mean average deviations are deemed unrealistically small, not reflecting realistic $\delta^{11}\text{B}$ discrepancies between individual laboratories, while the robust standard deviation better illustrates the scatter in the data sets (Figure 4). Table 5 summarises the various statistic results and Table 6 provides a list of the laboratories that submitted data.

Discussion

Overall, the agreement in $\delta^{11}\text{B}$ values reported here is very encouraging. Our BIIP dataset demonstrates that differences between the individual laboratories taking part in this study are orders of magnitude smaller than in earlier interlaboratory comparison efforts (Gonfiantini *et al.* 2003, Aggarwal *et al.* 2009, Foster *et al.* 2013). The slightly expanded robust standard deviation for JCt-1 ($2s^*$ of 0.60‰ for un-oxidised vs. 0.38‰ for oxidised powders) compared with the respective robust standard deviation for JCp-1 (0.45‰, un-oxidised vs. 0.22‰ for oxidised materials) is likely attributable to lower B/Ca in JCt-1 ($\sim 191 \mu\text{mol mol}^{-1}$) compared with JCp-1 ($\sim 460 \mu\text{mol mol}^{-1}$) (Hathorne *et al.* 2013), resulting in less favourable boron to matrix ratios. Besides the lower B content of JCt-1, several participating laboratories also reported that processing of this biogenic carbonate was not straightforward, particularly if samples were not oxidatively cleaned before elemental purification. Loading of un-oxidised JCt-1 solution onto the ion exchange columns in one laboratory even led to column blockages and resin needing to be discarded. The ionisation of un-oxidised JCt-1 equally posed significant challenges during N-TIMS measurement: since N-TIMS measures the $^{11}\text{BO}_2^-/^{10}\text{BO}_2^-$ ($m/z = 43$ relative to $m/z = 42$) ratio, organic matter (CNO) is known to interfere on $m/z = 42$ (Hemming and Hanson 1994) and therefore may explain the larger data variance in the measurement results in un-oxidised samples measured via N-TIMS.

Although detailed information on the behaviour of the two reference material powders during micro-sublimation purification is not available, results presented from the laboratory using this approach indicate slightly elevated measurement precisions for JCt-1 if no prior oxidative cleaning was performed ($2s$ of 0.37‰ for un-oxidised vs. 0.05‰ for oxidised reference materials). The purpose of exposing carbonates to an oxidative reagent is to remove carbonate-hosted organics (Boyle and Keigwin 1985). The observation that results are more reproducible for powder aliquots that underwent oxidative cleaning suggests that inconsistent results may at least in part be caused by organics present in the coral and giant clam carbonate matrix (Cuif and Dauphin 2005, Yoshimura *et al.* 2014). The observed improvement could either be controlled by removal of organically bound boron with a distinct isotopic signature during oxidative treatment, leading to more reproducible $\delta^{11}\text{B}$. Alternatively, since the oxidative treatment of biogenic carbonates often decreases the viscosity of the dissolved sample solution, this lowered viscosity should aid sample handling during elemental purification. Stewart *et al.* (2016) reported substantially lowered B/Ca for oxidised powders of JCp-1 (cleaned B/Ca of $325 \pm 2 \mu\text{mol mol}^{-1}$ vs. uncleaned B/Ca of $438 \pm 2 \mu\text{mol mol}^{-1}$; % RSD), suggesting removal of ~ 26 % boron during oxidative cleaning. At least some of the boron lost during oxidative treatment was likely of organic origin. However, although deemed possible, whether the organic fraction indeed yields a different isotopic composition compared with the carbonate fraction remains to be shown.

Oxidative treatment leads to better data agreement between various laboratories, yet our results suggest that aggressive bleaching (here using NaClO) of carbonate powders prior to analysis may result in undesired effects. While the $\delta^{11}\text{B}$ for un-oxidised reference materials provided by Laboratory 6 are in excellent agreement with the other datasets (z -scores of 0.88 for JCp-1 and -0.7 for JCt-1; see Tables 3 and 4), their reported oxidised $\delta^{11}\text{B}$ were identified as outliers. On the other hand, although the systematic shift in reported $\delta^{11}\text{B}$ for oxidatively cleaned materials from Laboratory 6 point towards the oxidative treatment in causing this effect, the oxidative cleaning protocol pursued by Laboratory 6 did not deviate substantially from those used in other laboratories, using NaClO at room temperature (Table 2). Hence the issue whether oxidative treatment indeed may cause fractionation of carbonate-hosted $\delta^{11}\text{B}$ cannot be resolved with the available data. Nevertheless, since oxidative cleaning improves the behaviour of boron on chromatographic resins and leads to better agreement of the measurement results between the

majority of laboratories, we recommend including this step (i.e., short exposure to buffered H₂O₂ or NaClO) for boron isotope analysis of biogenic carbonates.

Conclusions

Two biogenic marine carbonate reference materials from the Geological Survey of Japan (JCp-1 and JCt-1) were analysed for their boron isotopic ratio in ten laboratories with a documented record of prior boron isotope analyses. Compiled results reveal an encouragingly good agreement of the laboratory means between laboratories that is close to commonly reported in-house intermediate precisions. Since the vast majority of research groups participating in this study employed inductively coupled plasma-mass spectrometric approaches, the analytical assessment is somewhat biased towards these MC-ICP-MS approaches. Nevertheless, several general key conclusions can be drawn that also apply to thermal ionisation mass spectrometric approaches.

More consistent boron isotope results are obtained if carbonate materials were exposed to moderate oxidative treatment prior to sample dissolution. While utmost care in sample handling for boron isotopic studies is always required, the analytical approach taken for extracting boron from the carbonate matrix, as well as the sample introduction system used for MC-ICP-MS approaches, does not lead to resolvable isotope offsets. Following the oxidative cleaning approach, reported $\delta^{11}\text{B}$ for JCt-1 agrees to within $\pm 0.38\text{‰}$, and $\pm 0.22\text{‰}$ for JCp-1 ($2s^*$).

Given that future research efforts will tend to focus on smaller sample sizes and/or carbonates with low B/Ca, one of the most pressing pre-requisites for generating accurate $\delta^{11}\text{B}$ will be sustained or improved boron total procedural blank levels. The increased use of $10^{12}\Omega$ (Anagnostou *et al.* 2019, Jurikova *et al.* 2019) or even $10^{13}\Omega$ resistors (Lloyd *et al.* 2018) should equally help in generating boron isotopic data that are comparable between different laboratories even for small sample sizes in a few nanograms of boron. Finally, we note that despite the increasing levels of inter-laboratory consistency, boron isotope measurements remain challenging, even for those laboratories that have been making these measurements for many years. However, our study highlights that with care and commitment, it is possible to achieve a very encouraging level of consistency within the community.

Data availability statement and conflict of interest

All data presented and discussed in this study are presented in Tables 2 and 3. The authors declare no conflict of interest. Concise constructive criticism provided by two reviewers and the managing editor Thomas Meisel improved an earlier version of the manuscript and is greatly acknowledged.

References

13528:2015(E) I. (2015)

Statistical methods for use in proficiency testing by interlaboratory comparison. **International Organization for Standardization**, 90pp.

Aggarwal J., Böhm F., Foster G., Halas S., Honisch B., Jiang S.-Y., Kosler J., Liba A., Rodushkin I., Sheehan T., Jiun-San Shen J., Tonarini S., Xie Q., You C.-F., Zhao Z.-Q. and Zuleger E. (2009)

How well do non-traditional stable isotope results compare between different laboratories: Results from the interlaboratory comparison of boron isotope measurements. **Journal of Analytical Atomic Spectrometry**, **24**, 825–831.

Allison N., Finch A.A. and Eimf (2010)

Delta B-11, Sr, Mg and B in a modern porites coral: The relationship between calcification site pH and skeletal chemistry. **Geochimica et Cosmochimica Acta**, **74**, 1790–1800.

Anagnostou E., Williams B., Westfield I., Foster G.L. and Ries J.B. (2019)

Calibration of the pH- $\delta^{11}\text{B}$ and temperature-Mg/Li proxies in the long-lived high-latitude crustose coralline red alga *Clathromorphum compactum* via controlled laboratory experiments. **Geochimica et Cosmochimica Acta**, **254**, 142–155.

Balz R., Brändle U., Kämmerer E., Köhnlein D., Lutz O. and Nolle A. (1986)

^{11}B and ^{10}B NMR Investigations in aqueous solutions. **Zeitschrift für Naturforschung A**, **41**, 737–742.

Barker S., Greaves M. and Elderfield H. (2003)

A study of cleaning procedures used for foraminiferal Mg/Ca paleothermometry. **Geochemistry Geophysics Geosystems**, **4**, Art. No. 8407.

Boyle E.A. (1981)

Cadmium, zinc, copper, and barium in foraminifera tests. **Earth and Planetary Science Letters**, **53**, 11–35.

Boyle E.A. and Keigwin L.D. (1985)

Comparison of Atlantic and Pacific paleochemical records for the last 215,000 years – Changes in deep ocean circulation and chemical inventories. **Earth and Planetary Science Letters**, **76**, 135–150.

Cornwall C.E., Comeau S. and McCulloch M.T. (2017)

Coralline algae elevate pH at the site of calcification under ocean acidification. **Global Change Biology**, **23**, 4245–4256.

Cuif J.-P. and Dauphin Y. (2005)

The two-step mode of growth in the scleractinian coral skeletons from the micrometre to the overall scale. **Journal of Structural Biology**, **150**, 319–331.

Dickson A.G. (1990)

Thermodynamics of the dissociation of boric-acid in synthetic seawater from 273.15 K to 318.15 K. **Deep-Sea Research Part A**, **37**, 755–766.

Donald H.K., Ries J.B., Stewart J.A., Fowell S.E. and Foster G.L. (2017)

Boron isotope sensitivity to seawater pH change in a species of *Neogoniolithon* coralline red alga. **Geochimica et Cosmochimica Acta**, **217**, 240–253.

Douville E., Paterne M., Cabioch G., Louvat P., Gaillardet J., Juillet-Leclerc A. and Ayliffe L. (2010)

Abrupt sea surface pH change at the end of the Younger Dryas in the central sub-equatorial Pacific inferred from boron isotope abundance in corals (*Porites*). **Biogeosciences**, **7**, 2445–2459.

Farmer J.R., Hönisch B. and Uchikawa J. (2016)

Single laboratory comparison of MC-ICP-MS and N-TIMS boron isotope analyses in marine carbonates. **Chemical Geology**, **447**, 173–182.

Foster G.L. (2008)

Seawater pH, $p\text{CO}_2$ and $[\text{CO}_3^{2-}]$ variations in the Caribbean Sea over the last 130 kyr: A boron isotope and B/Ca study of planktic foraminifera. **Earth and Planetary Science Letters**, **271**, 254–266.

Foster G.L., Hönisch B., Paris G., Dwyer G.S., Rae J.W.B., Elliott T., Gaillardet J., Hemming N.G., Louvat P. and Vengosh A. (2013)

Interlaboratory comparison of boron isotope analyses of boric acid, seawater and marine CaCO_3 by MC-ICP-MS and N-TIMS. **Chemical Geology**, **358**, 1–14.

Foster G.L., Pogge von Strandmann P.A.E. and Rae J.W.B. (2010)

Boron and magnesium isotopic composition of seawater. **Geochemistry Geophysics Geosystems**, **11**, Art. No. Q08015.

Gonfiantini R., Tonarini S., Groning M., Adorni-Braccesi A., Al-Ammar A.S., Astner M., Bachler S., Barnes R.M., Bassett R.L., Cocherie A., Deyhle A., Dini A., Ferrara G., Gaillardet J., Grimm J., Guerrot C., Krahenbuhl U., Layne G., Lemarchand D., Meixner A., Northington D.J., Pennisi M., Reitznerova E., Rodushkin I., Sugiura N., Surberg R., Tonn S., Wiedenbeck M., Wunderli S., Xiao Y.K. and Zack T. (2003) Intercomparison of boron isotope and concentration measurements. Part II: Evaluation of results. **Geostandards Newsletter: The Journal of Geostandards and Geoanalysis**, **27**, 41–57.

Hathorne E., Gagnon A., Felis T., Adkins J., Asami R., Boer W., Caillon N., Case D., Cobb K.M., Douville E., deMenocal P., Eisenhauer A., Garbe-Schönberg D., Geibert W., Goldstein S., Hughen K., Inoue M., Kawahata H., Kölling M., Cornec F.L., Linsley B.K., McGregor H.V., Montagna P., Nurhati I.S., Quinn T.M., Raddatz J., Rebaubier H.e., Robinson L., Sadekov A., Sherrell R., Sinclair D., Tudhope A.W., Wei G., Wong H., Wu H.C. and You C.-F. (2013) Interlaboratory study for coral Sr/Ca and other element/Ca ratio measurements. **Geochemistry Geophysics Geosystems**, **14**, 3730–3750.

Heinemann A., Fietzke J., Melzner F., Boehm F., Thomsen J., Garbe-Schoenberg D. and Eisenhauer A. (2012) Conditions of *Mytilus edulis* extracellular body fluids and shell composition in a pH-treatment experiment: Acid-base status, trace elements and $\delta^{11}\text{B}$. **Geochemistry Geophysics Geosystems**, **13**, Art. No. Q01005.

Hemming N.G. and Hanson G.N. (1992) Boron isotopic composition and concentration in modern marine carbonates. **Geochimica et Cosmochimica Acta**, **56**, 537–543.

Hemming N.G. and Hanson G.N. (1994) A procedure for the isotopic analysis of boron by negative thermal ionization mass-spectrometry. **Chemical Geology**, **114**, 147–156.

Hönisch B. and Hemming N.G. (2005) Surface ocean pH response to variations in $p\text{CO}_2$ through two full glacial cycles. **Earth and Planetary Science Letters**, **236**, 305–314.

Hönisch B., Hemming N.G., Grottoli A.G., Amat A., Hanson G.N. and Buma J. (2004) Assessing scleractinian corals as recorders for paleo-pH: Empirical calibration and vital effects. **Geochimica et Cosmochimica Acta**, **68**, 3675–3685.

Inoue M., Nohara M., Okai T., Suzuki A. and Kawahata H. (2004) Concentrations of trace elements in carbonate reference materials coral JCp-1 and giant clam JCt-1 by inductively coupled plasma-mass spectrometry. **Geostandards and Geoanalytical Research**, **28**, 411–416.

Jurikova H., Liebetrau V., Gutjahr M., Rollion-Bard C., Hu M.Y., Krause S., Henkel D., Hiebenthal C., Schmidt M., Laudien J. and Eisenhauer A. (2019)

Boron isotope systematics of cultured brachiopods: Response to acidification, vital effects and implications for palaeo-pH reconstruction. **Geochimica et Cosmochimica Acta**, **248**, 370–386.

Klochko K., Kaufman A.J., Yao W.S., Byrne R.H. and Tossell J.A. (2006)

Experimental measurement of boron isotope fractionation in seawater. **Earth and Planetary Science Letters**, **248**, 276–285.

Lazareth C.E., Soares-Pereira C., Douville E., Brahmi C., Dissard D., Le Cornec F., Thil F., Gonzalez-Roubaud C., Caquineau S. and Cabioch G. (2016)

Intra-skeletal calcite in a live-collected *Porites* sp.: Impact on environmental proxies and potential formation process. **Geochimica et Cosmochimica Acta**, **176**, 279–294.

Lecuyer C., Grandjean P., Reynard B., Albarède F. and Télouk P. (2002)

$^{11}\text{B}/^{10}\text{B}$ analysis of geological materials by ICP-MS Plasma 54: Application to the boron fractionation between brachiopod calcite and seawater. **Chemical Geology**, **186**, 45–55.

Lemarchand D., Gaillardet J., Lewin E. and Allègre C.J. (2000)

The influence of rivers on marine boron isotopes and implications for reconstructing past ocean pH. **Nature**, **408**, 951–954.

Lloyd N.S., Sadekov A.Y. and Misra S. (2018)

Application of 10^{13} ohm Faraday cup current amplifiers for boron isotopic analyses by solution mode and laser ablation multicollector inductively coupled plasma mass spectrometry. **Rapid Communications in Mass Spectrometry**, **32**, 9–18.

Louvat P., Bouchez J. and Paris G. (2011)

MC-ICP-MS isotope measurements with direct injection nebulisation (d-DIHEN): Optimisation and application to boron in seawater and carbonate samples. **Geostandards and Geoanalytical Research**, **35**, 75–88.

Louvat P., Moureau J., Paris G., Bouchez J., Noireaux J. and Gaillardet J. (2014)

A fully automated direct injection nebulizer (d-DIHEN) for MC-ICP-MS isotope analysis: Application to boron isotope ratio measurements. **Journal of Analytical Atomic Spectrometry**, **29**, 1698–1707.

McCulloch M., Falter J., Trotter J. and Montagna P. (2012)

Coral resilience to ocean acidification and global warming through pH up-regulation. **Nature Climate Change**, **2**, 623–627.

McCulloch M.T., Holcomb M., Rankenburg K. and Trotter J.A. (2014)

Rapid, high-precision measurements of boron isotopic compositions in marine carbonates. **Rapid Communications in Mass Spectrometry**, **28**, 2704–2712.

Misra S., Owen R., Kerr J., Greaves M. and Elderfield H. (2014)

Determination of $\delta^{11}\text{B}$ by HR-ICP-MS from mass limited samples: Application to natural carbonates and water samples. **Geochimica et Cosmochimica Acta**, **140**, 531–552.

Oi T., Kato J., Ossaka T. and Kakihana H. (1991)

Boron isotope fractionation accompanying boron mineral formation from aqueous boric acid-sodium hydroxide solutions at 25 °C. **Geochemical Journal**, **25**, 377–385.

Okai T., Suzuki A., Kawahata H., Terashima S. and Imai N. (2002)

Preparation of a new Geological Survey of Japan geochemical reference material: Coral JCP-1. **Geostandards Newsletter: The Journal of Geostandards and Geoanalysis**, **26**, 95–99.

Okai T., Suzuki A., Terashima S., Inoue M., Nohara M., Kawahata H. and Imai N. (2004)

Collaborative analysis of GSJ/AIST geochemical reference materials JCP 1 (Coral) and JCt 1 (Giant Clam). **Geochemistry Geophysics Geosystems**, **38**, 281–286.

Paris G., Bartolini A., Donnadiou Y., Beaumont V. and Gaillardet J. (2010)

Investigating boron isotopes in a middle Jurassic micritic sequence: Primary vs. diagenetic signal. **Chemical Geology**, **275**, 117–126.

Penman D.E., Hönisch B., Rasbury E.T., Hemming N.G. and Spero H.J. (2013)

Boron, carbon, and oxygen isotopic composition of brachiopod shells: Intra-shell variability, controls, and potential as a paleo-pH recorder. **Chemical Geology**, **340**, 32–39.

Raddatz J., Liebetrau V., Trotter J., Rüggeberg A., Flögel S., Dullo W.-C., Eisenhauer A., Voigt S. and McCulloch M. (2016)

Environmental constraints on Holocene cold-water coral reef growth off Norway: Insights from a multiproxy approach. **Paleoceanography**, **31**, 1350–1367.

Rae J.W.B., Burke A., Robinson L.F., Adkins J.F., Chen T., Cole C., Greenop R., Li T., Little E.F.M., Nita D.C., Stewart J.A. and Taylor B.J. (2018)

CO₂ storage and release in the deep Southern Ocean on millennial to centennial timescales. **Nature**, **562**, 569–573.

Rae J.W.B., Foster G.L., Schmidt D.N. and Elliott T. (2011)

Boron isotopes and B/Ca in benthic foraminifera: Proxies for the deep ocean carbonate system. **Earth and Planetary Science Letters**, **302**, 403–413.

Reynaud S., Hemming N.G., Juillet-Leclerc A. and Gattuso J.P. (2004)

Effect of $p\text{CO}_2$ and temperature on the boron isotopic composition of the zooxanthellate coral *Acropora* sp. **Coral Reefs**, **23**, 539–546.

Rollion-Bard C., Chaussidon M. and France-Lanord C. (2003)

pH control on oxygen isotopic composition of symbiotic corals. **Earth and Planetary Science Letters**, **215**, 275–288.

Rosner M., Romer R.L. and Meixner A. (2005)

Air handling in clean laboratory environments: The reason for anomalously high boron background levels. **Analytical and Bioanalytical Chemistry**, **382**, 120–124.

Roux P., Lemarchand D., Hughes H.J. and Turpault M.P. (2015)

A rapid method for determining boron concentration (ID-ICP-MS) and $\delta^{11}\text{B}$ (MC-ICP-MS) in vegetation samples after microwave digestion and cation exchange chemical purification. **Geostandards and Geoanalytical Research**, **39**, 453–466.

Srnková J. and Zbíral J. (2009)

Comparison of different approaches to the statistical evaluation of proficiency tests. **Accreditation and Quality Assurance**, **14**, 467–471.

Stewart A.J., Day R.D., Christopher S.J., Kucklick J.R., Bordier L., Chalk T.B., Dapoigny A., Douville E., Foster G.L., Gray W.R., Greenop R., Gutjahr M., Hemsing F., Henahan M.J., Holdship P., Hsieh Y.-T., Kolečka A., Lin Y.-P., Mawbey E.M., Rae J.W.B., Robinson L.F., Shuttleworth R., You C.-F. and Zhang S. (2020 in press)

NIST RM 8301 Boron isotopes in marine carbonate (simulated coral and foraminifera solutions): Inter-laboratory $\delta^{11}\text{B}$ and trace metal ratio value assignment. **Geostandards and Geoanalytical Research**.

Stewart J.A., Anagnostou E. and Foster G.L. (2016)

An improved boron isotope pH proxy calibration for the deep-sea coral *Desmophyllum dianthus* through sub-sampling of fibrous aragonite. **Chemical Geology**, **447**, 148–160.

Vengosh A., Kolodny Y., Starinsky A., Chivas A.R. and McCulloch M.T. (1991)

Coprecipitation and isotopic fractionation of boron in modern biogenic carbonates. **Geochimica et Cosmochimica Acta**, **55**, 2901–2910.

Voinot A., Lemarchand D., Collignon C., Granet M., Chabaux F. and Turpault M.P. (2013)

Experimental dissolution vs. transformation of micas under acidic soil conditions: Clues from boron isotopes. **Geochimica et Cosmochimica Acta**, **117**, 144–160.

Wall M., Fietzke J., Schmidt G.M., Fink A., Hofmann L.C., de Beer D. and Fabricius K.E. (2016)

Internal pH regulation facilitates *in situ* long-term acclimation of massive corals to end-of-century carbon dioxide conditions. **Scientific Reports**, **6**, 30688.

Wang B.S., You C.F., Huang K.F., Wu S.F., Aggarwal S.K., Chung C.H. and Lin P.Y. (2010)

Direct separation of boron from Na- and Ca-rich matrices by sublimation for stable isotope measurement by MC-ICP-MS. **Talanta**, **82**, 1378–1384.

Wu H.C., Dissard D., Douville E., Blamart D., Bordier L., Tribollet A., Le Cornec F., Pons-Branchu E., Dapoigny A. and Lazareth C.E. (2018)

Surface ocean pH variations since 1689 CE and recent ocean acidification in the tropical South Pacific. **Nature Communications**, **9**, 2543.

Yoshimura T., Tamenori Y., Kawahata H. and Suzuki A. (2014)

Fluctuations of sulfate, S-bearing amino acids and magnesium in a giant clam shell. **Biogeosciences**, **11**, 3881–3886.

Zeebe R.E. (2005)

Stable boron isotope fractionation between dissolved $B(OH)_3$ and $B(OH)_4^-$. **Geochimica et Cosmochimica Acta**, **69**, 2753–2766.

Figure captions

Figure 1. Boron isotope results for modern *Porites* sp. coral JCp-1, presented in delta notation relative to NIST SRM 951, presenting the mean $\delta^{11}B$ for each laboratory with resultant $2s$ (see also Table 3) for (a) un-oxidised samples and (b) aliquots that underwent preceding oxidative treatment. Shaded area corresponds to the $\delta^{11}B$ range enclosed by the double robust standard deviation $2s^*$ (see text for discussion). Values for the robust mean and double robust standard deviation are equally displayed and indicated by the grey lines in (a) and (b). (c) z -score associated with the mean laboratory $\delta^{11}B$ compositions shown in (a). (d) z -score associated with the mean laboratory $\delta^{11}B$ compositions shown in (b). An absolute z -score below or equal to 2 is considered acceptable, absolute z -score values between 2 and 3 are of likely questionable quality, and absolute values beyond 3 suggest that results are outside the satisfactory range, as indicated by the stippled horizontal lines in (c) and (d).

Figure 2. Boron isotope results for *Tridacna gigas* JCt-1 reference material, presented in delta notation relative to NIST SRM 951, showing the mean $\delta^{11}\text{B}$ for each laboratory with resultant $2s$ (see also Table 4) for (a) un-oxidised samples and (b) aliquots that underwent prior oxidative treatment. Shaded area corresponds to the $\delta^{11}\text{B}$ range enclosed by the double robust standard deviation $2s^*$ (see text for discussion). Values for the robust mean and double robust standard deviation are equally displayed and indicated by the grey lines in (a) and (b). (c) and (d) show z -scores associated with the mean laboratory $\delta^{11}\text{B}$ values in (a) and (b) respectively.

Figure 3. Effect of sample ionisation/introduction system used, displaying results from three repeat samples per laboratory and cleaning protocol followed (cf. Tables 3 and 4 for data). Shown is the offset in measured individual $\delta^{11}\text{B}$ (three results per laboratory) from the respective interlaboratory robust mean. Symbols group data produced using (i) a quartz or (ii) PFA spray chamber, (iii) direct sample injection into the plasma, or (iv) thermal sample ionisation. Shaded area corresponds to the $\delta^{11}\text{B}$ measurement precision range enclosed by the double robust standard deviation $2s^*$ (see text for discussion). Note that the y -axis scales of panel (a) and (c) (JCp-1 un-oxidised/oxidised), as well as those for panels (b) and (d) (JCt-1 un-oxidised/oxidised) have been matched to allow better comparison between data sets.

Figure 4. Summary of robust mean $\delta^{11}\text{B}$ and robust standard deviation ($2s^*$) of (a) un-oxidised and (b) oxidised JCp-1 next to individual data provided by all laboratories, presented in delta notation relative to NIST SRM 951. (c) Comparison of un-oxidised and oxidised robust mean $\delta^{11}\text{B}$ data. (d, e, f) show the same comparisons for JCt-1. Note that panels (a) and (b) as well as panels (d) and (e) have the same y -axis scale for better comparability, while those for panels (c) and (f) are plotted at finer scale for the presentation of robust means including respective double robust standard deviation. The p -value of a two-sided Student's t -test is also shown for the respective data sets in panels (c) and (f).

Table 1.					
Selected previously published geochemical data from JCp-1 and Jct-1					
	JCp-1	2s	Jct-1	2s	Reference
CaO (% <i>m/m</i>)	53.50	0.28	54.66	0.16	Okai <i>et al.</i> (2004)
LOI (% <i>m/m</i>)	44.36	n.d.	44.27	n.d.	Okai <i>et al.</i> (2004)
<i>Robust means and robust std deviations reported below for previously unoxidised sample powders</i>					
Sr/Ca (mmol mol ⁻¹)	8.838	0.042	1.680	0.026	Hathorne <i>et al.</i> (2013)
Mg/Ca (mmol mol ⁻¹)	4.199	0.065	1.289	0.045	Hathorne <i>et al.</i> (2013)
U/Ca (nmol mol ⁻¹)	1192	0.045	22.71	2.40	Hathorne <i>et al.</i> (2013)
Ba/Ca (μmol mol ⁻¹)	7.465	0.655	4.348	0.280	Hathorne <i>et al.</i> (2013)
B/Ca (μmol mol ⁻¹)	459.6	22.7	191.0	9.3	Hathorne <i>et al.</i> (2013)
Li/Ca (μmol mol ⁻¹)	6.185	0.107	4.076	0.503	Hathorne <i>et al.</i> (2013)

Mass spectrometric approaches used and analytical details							
Mass spectrometry	Purification method	Oxidative reagent used	Exposure time to oxidative reagent	Temperature used during oxidative treatment	Sample introduction	Reference	Total procedural blank
MC-N-TIMS	none	O ₂ buffered in 0.1 mol l ⁻¹ NaOH: 1% (JCT-1) or 50% (JCP)	10 min (JCT-1); 2x30 min (JCP-1)	80 °C	ionisation from filament	Foster <i>et al.</i> (2013)	~ 10 pg
MC-ICP-MS	sublimation	6–14% NaClO	24 h	25 °C	quartz spray chamber	Wang <i>et al.</i> (2010)	< 8 pg
MC-ICP-MS	separation by ion exchange	10% H ₂ O ₂	8 min	25 °C	micro-cyclonic quartz spray chamber	Douville <i>et al.</i> (2010)	~ 500 pg
MC-ICP-MS	separation by ion exchange	10% H ₂ O ₂ buffered to pH 9 with NH ₄ OH	1 h	25 °C	direct injection (δ-DIHEN)	Louvat <i>et al.</i> (2011, 2014), Paris <i>et al.</i> (2010)	~ 150 pg
MC-ICP-MS	separation by ion exchange	buffered 1% H ₂ O ₂	15 min (i.e. 3 x 5 min u/s in between)	80 °C	PFA scott spray chamber	Foster (2008), Rae <i>et al.</i> (2011, 2018)	~ 92 pg
MC-ICP-MS	separation by ion exchange	n.a.	n.a.	n.a.	mini cyclonic quartz spray chamber	Gonfiantini <i>et al.</i> (2003), Aggarwal <i>et al.</i> (2009)	~ 500 pg
MC-ICP-MS	separation by ion exchange	NaClO ₂ 5% Cl	15 h	21 °C	mini cyclonic quartz spray chamber	Foster (2008), Voinot <i>et al.</i> (2013)	~ 3000 pg
MC-ICP-MS	separation by ion exchange	buffered 1% H ₂ O ₂	15 min (i.e. 3 x 5 min u/s in between)	80 °C	PFA scott spray chamber	Foster (2008), Rae <i>et al.</i> (2011)	~ 28 pg
MC-ICP-MS	separation by ion exchange	buffered 1% H ₂ O ₂	15 min (i.e. 3 x 5 min u/s in between)	80 °C	PFA scott spray chamber	Foster (2008), Rae <i>et al.</i> (2011)	~ 240 pg
MC-ICP-MS	separation by ion exchange	NaClO	15 min	25 °C	quartz spray chamber	McCulloch <i>et al.</i> (2014)	~ 500 pg

[illegible]

Lab ID	Replicate type / number	Replicate mean $\bar{S}^{1/2}$	2s	n ⁽¹⁾	Amount used (mg)	Lab mean $\bar{S}^{1/2}$	laboratory 2s (n = 3)	z score	robust mean	Lab ID	Replicate type / number	Replicate mean $\bar{S}^{1/2}$	2s	n ⁽¹⁾	Amount used (mg)	Lab mean $\bar{S}^{1/2}$	laboratory 2s (n = 3)	z score	robust mean	$\Delta \bar{S}^{1/2}$ (oxidised-un-oxidised)
A	un-oxidised A	24.63	0.08	3	23.7					A	oxidised A	23.95	0.22	3	17.8					
A	un-oxidised B	24.66	0.11	3	18.3	24.71	0.24	1.55	0.35	A	oxidised B	24.07	0.20	3	21.6	24.11	0.32	-1.25	-0.13	-0.60
A	un-oxidised C	24.85	0.18	3	20.3					A	oxidised C	24.27	0.12	3	17.6					
B	un-oxidised A	24.45	0.04	3	9.6	24.39	0.12	0.12	0.03	B	oxidised A	24.18	0.06	3	5.50	24.19	0.03	-0.51	-0.05	-0.20
B	un-oxidised B	24.34	0.06	3	7.2					B	oxidised B	24.21	0.15	3	6.40					
B	un-oxidised C	24.37	0.09	3	5.6					B	oxidised C	24.14	0.14	3	7.80					
C	un-oxidised A	24.12	0.26	3	6.2					C	oxidised A	24.16	0.29	3	6.41					
C	un-oxidised B	24.03	0.26	3	6.5	24.09	0.11	-1.21	-0.27	C	oxidised B	24.21	0.29	3	7.28	24.20	0.07	-0.42	-0.04	0.11
C	un-oxidised C	24.12	0.15	3	6.2					C	oxidised C	24.22	0.23	3	6.40					
D	un-oxidised A	22.49	0.13	3	200					D	oxidised A	n.d.								
D	un-oxidised B	22.57	0.56	3	200	22.57	0.15	-7.92	-1.80	D	oxidised B	n.d.								
D	un-oxidised C	22.64	0.40	3	200					D	oxidised C	n.d.								
E	un-oxidised A	24.28	0.11	5	99					E	oxidised A	24.25	0.22	5	97.0					
E	un-oxidised B	24.32	0.16	5	102	24.32	0.08	-0.18	-0.04	E	oxidised B	24.20	0.18	5	98.6	24.27	0.15	0.23	0.02	-0.05
E	un-oxidised C	24.36	0.19	5	103					E	oxidised C	24.35	0.07	5	99.7					
F	un-oxidised A	24.72	0.26	4	50					F	oxidised A	23.72	0.24	4	50					
F	un-oxidised B	24.57	0.17	4	50	24.56	0.31	0.88	0.20	F	oxidised B	23.75	0.14	4	50	23.82	0.32	-3.93	-0.42	-0.74
F	un-oxidised C	24.41	0.16	4	50					F	oxidised C	24.01	0.15	4	50					
G	un-oxidised A	24.31	0.20	2	10	24.36	0.15	-0.01	0.00	G	oxidised A	24.20	0.20	2	10					
G	un-oxidised B	24.32	0.20	2	10					G	oxidised B	24.37	0.20	2	10	24.33	0.23	0.82	0.09	-0.03
G	un-oxidised C	24.45	0.20	2	10					G	oxidised C	24.43	0.20	2	10					
H	un-oxidised A	24.46	0.12	4	10.2					H	oxidised A	24.36	0.02	3	10.1					
H	un-oxidised B	24.37	0.16	4	11.9	24.46	0.18	0.42	0.10	H	oxidised B	24.41	0.21	4	9.70	24.38	0.06	1.29	0.14	-0.07
H	un-oxidised C	24.55	0.12	4	12.4					H	oxidised C	24.38	0.18	4	9.55					
I	un-oxidised A	24.48	0.11	3	10					I	oxidised A	24.36	0.23	3	10					
I	un-oxidised B	24.46	0.07	4	10	24.49	0.07	0.55	0.13	I	oxidised B	24.24	0.16	3	10	24.30	0.12	0.52	0.06	-0.

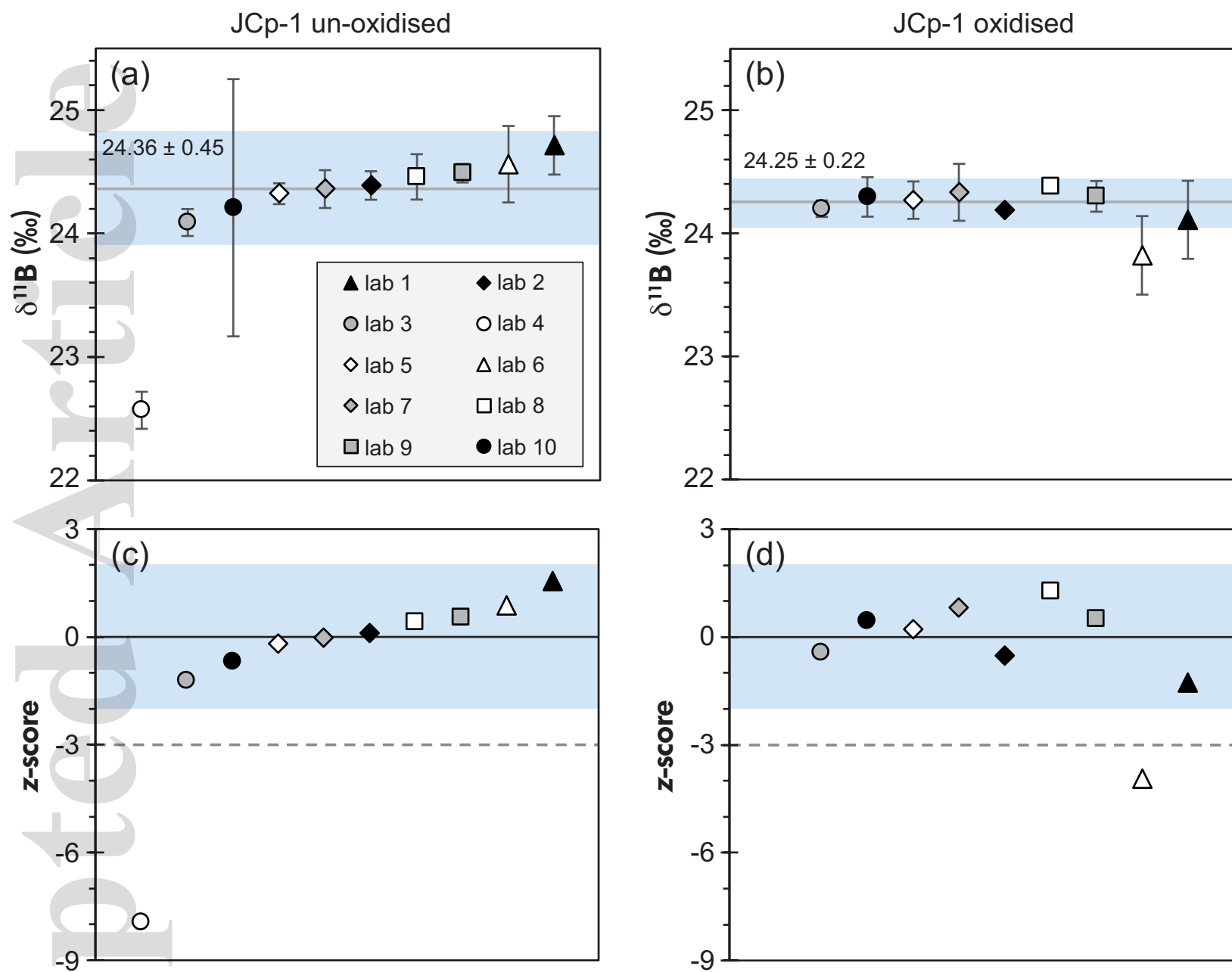
Table 4.																				
JC-1 reference material results (un-oxidised and oxidised)																				
Lab ID	Replicate type / number	Replicate mean $\delta^{13}\text{C}$	2s	n ⁽¹⁾	Amount used (mg)	Lab mean $\delta^{13}\text{C}$	laboratory 2s (n = 3), z score	robust mean	Lab ID	Replicate type / number	Replicate mean $\delta^{13}\text{C}$	2s	n ⁽¹⁾	Amount used (mg)	Lab mean $\delta^{13}\text{C}$	laboratory 2s (n = 3), z score	robust mean	$\Delta\delta^{13}\text{C}$ (oxidised-un-oxidised)		
A	un-oxidised A	16.33	0.12	3	15.1				A	oxidised A	16.37	0.21	3	17.8						
A	un-oxidised B	16.04	0.09	3	13.7	16.35	0.63	-0.14	-0.04	A	oxidised B	15.94	0.50	3	19.0	16.03	0.58	-1.10	-0.21	-0.32
A	un-oxidised C	16.67	0.09	3	13.5					A	oxidised C	15.82	0.14	3	18.4					
B	un-oxidised A	n.d.							B	oxidised A	16.15	0.13	3	7.60						
B	un-oxidised B	n.d.							B	oxidised B	16.24	0.05	3	7.00	16.21	0.11	-0.14	-0.03		
B	un-oxidised C	n.d.							B	oxidised C	16.25	0.14	3	6.20						
C	un-oxidised A	16.28	0.17	3	6.50				C	oxidised A	16.24	0.29	3	6.24						
C	un-oxidised B	16.16	0.45	3	6.34	16.12	0.37	-0.90	-0.27	C	oxidised B	16.18	0.41	3	6.29	16.21	0.05	-0.15	-0.03	0.09
C	un-oxidised C	15.92	0.06	3	6.76					C	oxidised C	16.20	0.18	3	5.80					
D	un-oxidised A	15.43	0.25	3	200				D	oxidised A	n.d.									
D	un-oxidised B	15.34	0.48	3	200	15.32	0.23	-3.58	-1.07	D	oxidised B	n.d.								
D	un-oxidised C	15.20	0.13	3	200					D	oxidised C	n.d.								
E	un-oxidised A	16.29	0.17	5	201				E	oxidised A	16.16	0.16	5	198						
E	un-oxidised B	16.39	0.04	5	204	16.33	0.11	-0.18	-0.05	E	oxidised B	16.25	0.19	5	199	16.29	0.30	0.25	0.05	-0.05
E	un-oxidised C	16.31	0.05	5	200					E	oxidised C	16.45	0.17	5	201					
F	un-oxidised A	16.11	0.26	4	50				F	oxidised A	14.97	0.17	4	50						
F	un-oxidised B	16.12	0.23	4	50	16.18	0.23	-0.70	-0.21	F	oxidised B	14.91	0.19	4	50	15.01	0.23	-6.41	-1.23	-1.17
F	un-oxidised C	16.31	0.18	4	50					F	oxidised C	15.14	0.18	4	50					
G	un-oxidised A	16.60	0.20	2	20				G	oxidised A	16.28	0.20	2	20						
G	un-oxidised B	16.51	0.20	2	20	16.47	0.32	0.27	0.08	G	oxidised B	16.36	0.20	2	20	16.21	0.37	-0.12	-0.02	-0.25
G	un-oxidised C	16.29	0.20	2	20					G	oxidised C	16.01	0.20	2	20					
H	un-oxidised A	16.53	0.21	4	10.17					H	oxidised A	16.40	0.27	3	11.2					
H	un-oxidised B	16.55	0.29	4	12.78	16.56	0.06	0.57	0.17	H	oxidised B	16.50	0.23	3	10.7	16.43	0.11	1.03	0.20	-0.12
H	un-oxidised C	16.59	0.28	4	12.52					H	oxidised C	16.41	0.16	3	11.7					
I	un-oxidised A	16.44	0.06	4	10					I	oxidised A	16.33	0.18	3	10					
I	un-oxidised B	16.37	0.12	4	10	16.41	0.08	0.10	0.03	I	oxidised B	16.23	0.21	3	10	16.33	0.20	0.48	0.09	-0.09
I	un-oxidised C	16.44	0.15	3	10					I	oxidised C	16.43	0.28	3	10					
J	un-oxidised A	17.26	0.31	10	7.17					J	oxidised A	16.98	0.21	10	6.75					
J	un-oxidised B	17.06	0.19	10	6.21	16.89	0.96	1.70	0.50	J	oxidised B	16.63	0.23	10	8.59	16.68	0.57	2.28	0.44	-0.22
J	un-oxidised C	16.35	0.20	10	5.29					J	oxidised C	16.42	0.28	10	3.69					

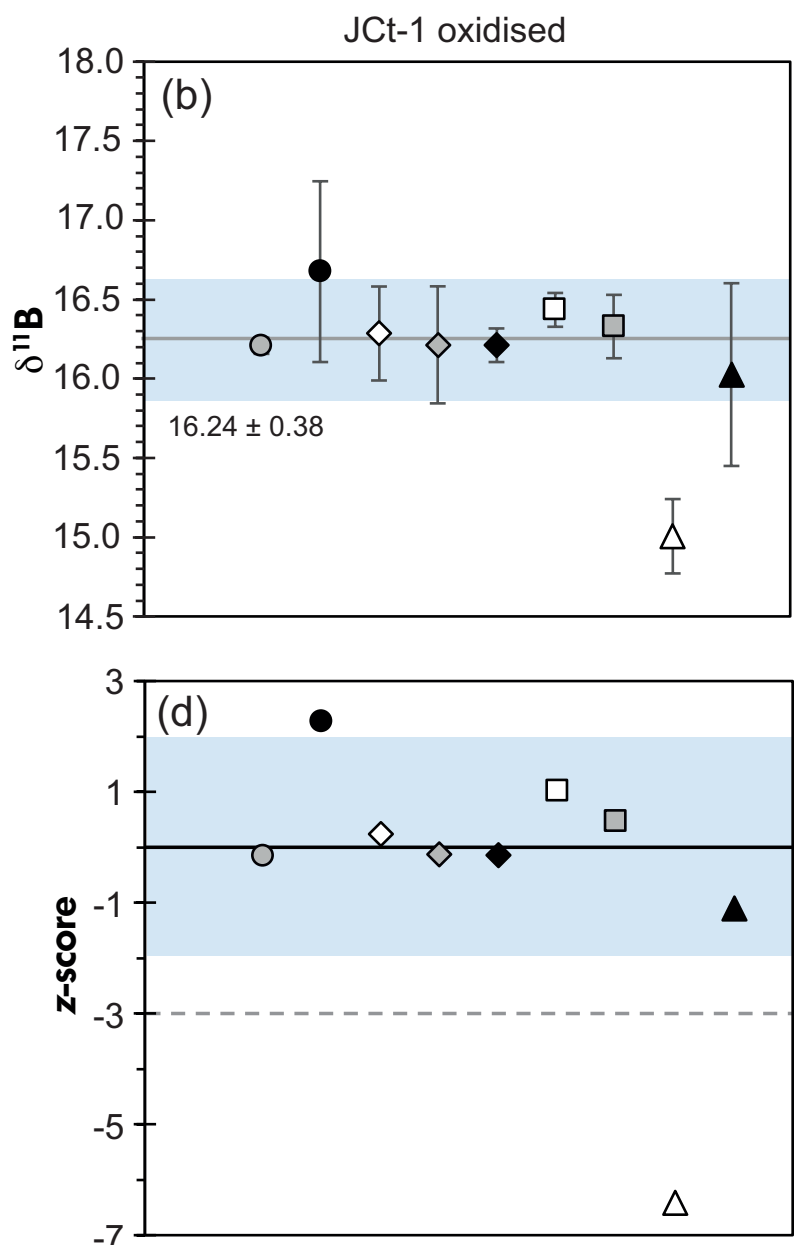
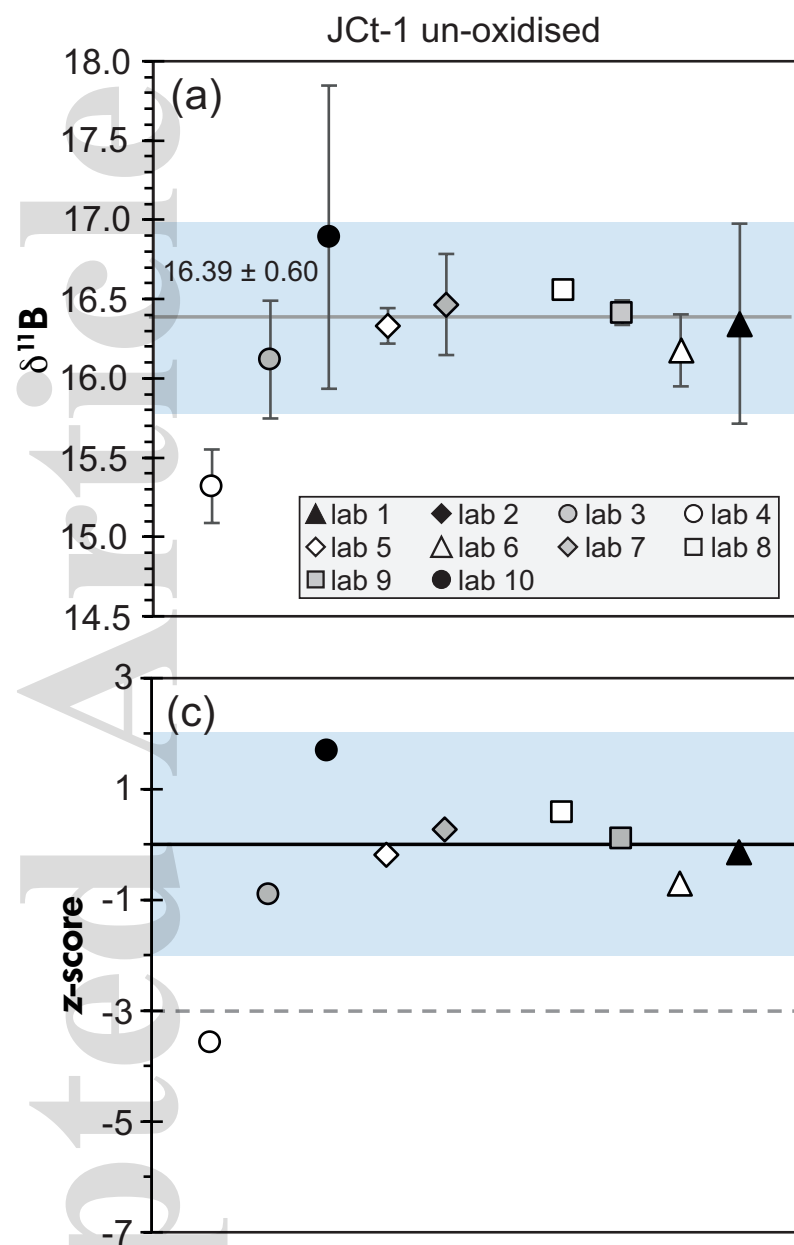
Table 5.						
Summary for JCp-1 and Jct-1 reference materials of intercalibration routine						
JCp-1 non-oxidised				JCp-1 oxidised		
	$\delta^{11}\text{B}$		n		$\delta^{11}\text{B}$	n
robust mean and corresponding 2s*	24.36	0.45	10	24.25	0.22	9
median of laboratory averages with mean average deviation	24.37	0.31	10	24.27	0.11	9
median of individual results with mean average deviation	24.37	0.34	30	24.22	0.12	27
Jct-1 non-oxidised				Jct-1 oxidised		
	$\delta^{11}\text{B}$		n		$\delta^{11}\text{B}$	n
robust mean and corresponding 2s*	16.39	0.60	9	16.24	0.38	9
median of laboratory averages with mean average deviation	16.35	0.26	9	16.21	0.25	9
median of individual results with mean average deviation	16.33	0.30	27	16.25	0.28	27

Table 6.**List of laboratories that submitted results to the BIIP study**

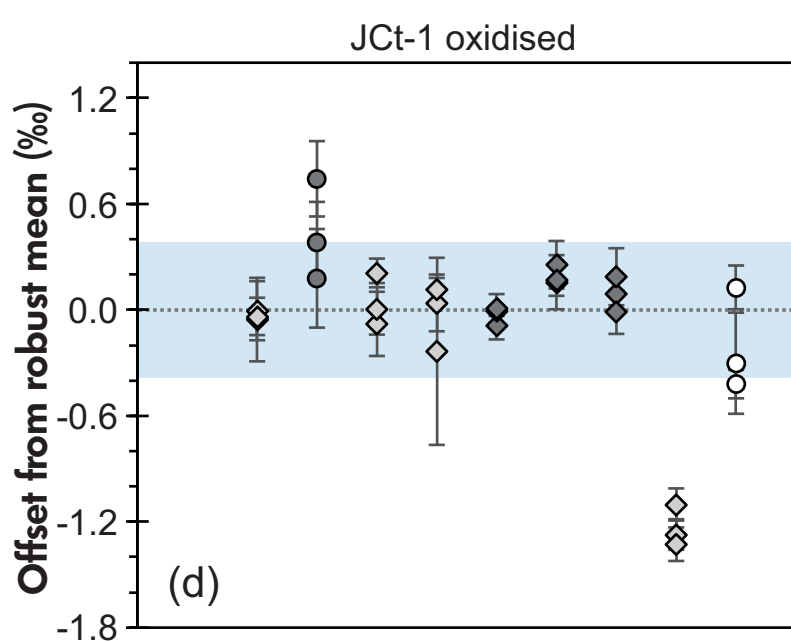
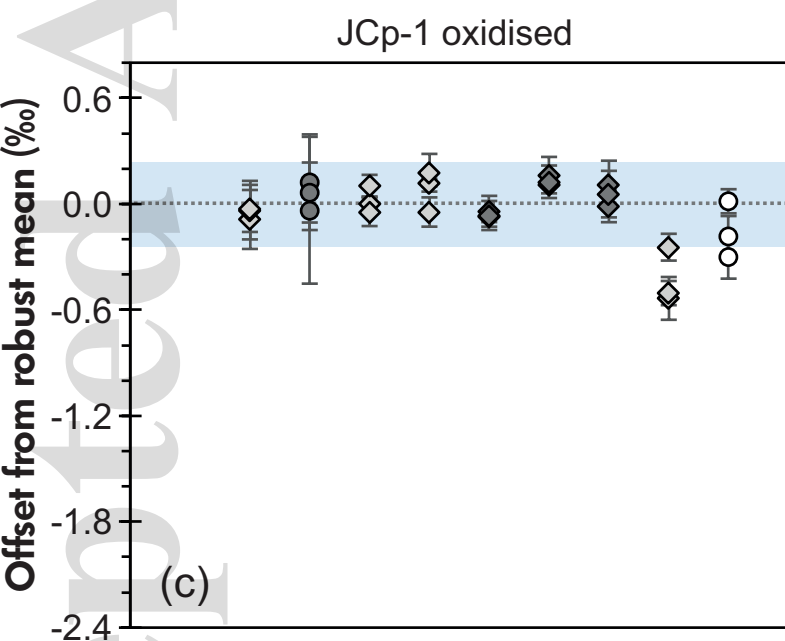
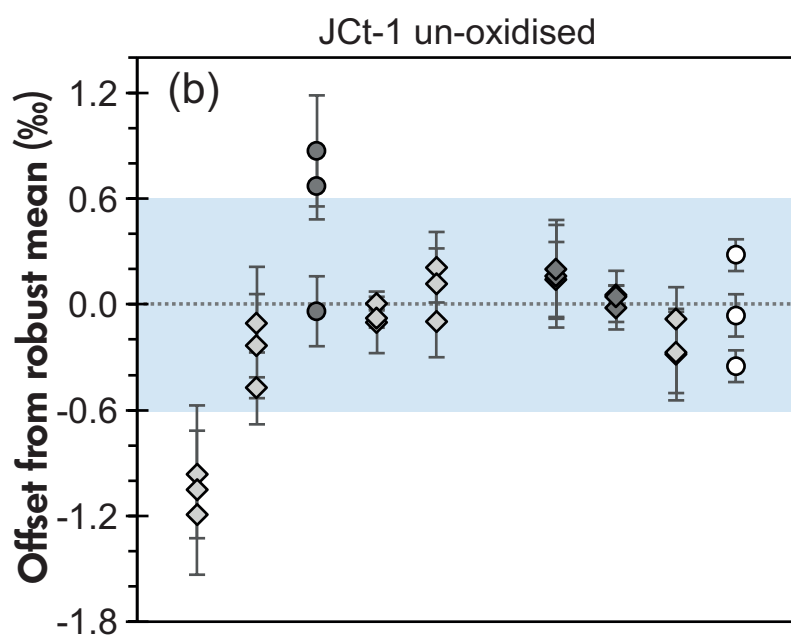
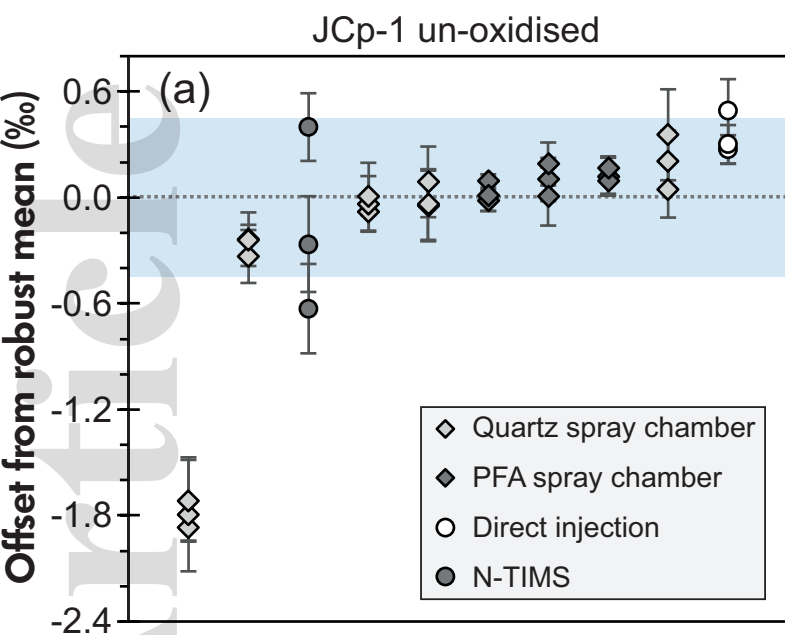
I	Isotope Geochemistry Laboratory, Department of Earth Sciences, National Cheng Kung University, No 1 University Road, 701 Tainan, Taiwan
II	Laboratoire des Sciences du Climat et de l'Environnement, LSCE/IPSL, CEA-CNRS-UVSQ, Université Paris-Saclay, F-91191 Gif-sur-Yvette, France
III	Institut de Physique du Globe de Paris, Sorbonne Paris Cité, Université Paris-Diderot, UMR CNRS 7154, 1 rue Jussieu, 75238 Paris Cedex 05, France
IV	School of Earth and Environmental Sciences, University of St Andrews, North Street, St Andrews, UK
VI	Department of Earth and Environmental Sciences and Lamont-Doherty Earth Observatory of Columbia University 61 Route 9W Palisades, NY 10964, U.S.A.
VII	ALS Scandinavia AB, Aurorum 10, SE-97775 Luleå, Sweden
VIII	Laboratoire d'Hydrologie et de Géochimie de Strasbourg, EOST, Université de Strasbourg et CNRS, 1 rue Blessig, 67084 Strasbourg, France
IX	School of Ocean and Earth Science, University of Southampton, National Oceanography Centre, Southampton, European Way, Southampton SO14 3ZH, UK
X	Geological and Planetary Sciences, Caltech, 1200 E California Blvd, Pasadena, California, 91125, U.S.A.
XI	ARC Centre of Excellence for Coral Reef Studies and School of Earth and Environment, The University of Western Australia, Crawley 6009, Australia

Note that the order of laboratories here does not correspond to the order of laboratory numbers in Tables 3 and 4, as well as Figures 1 to 3.

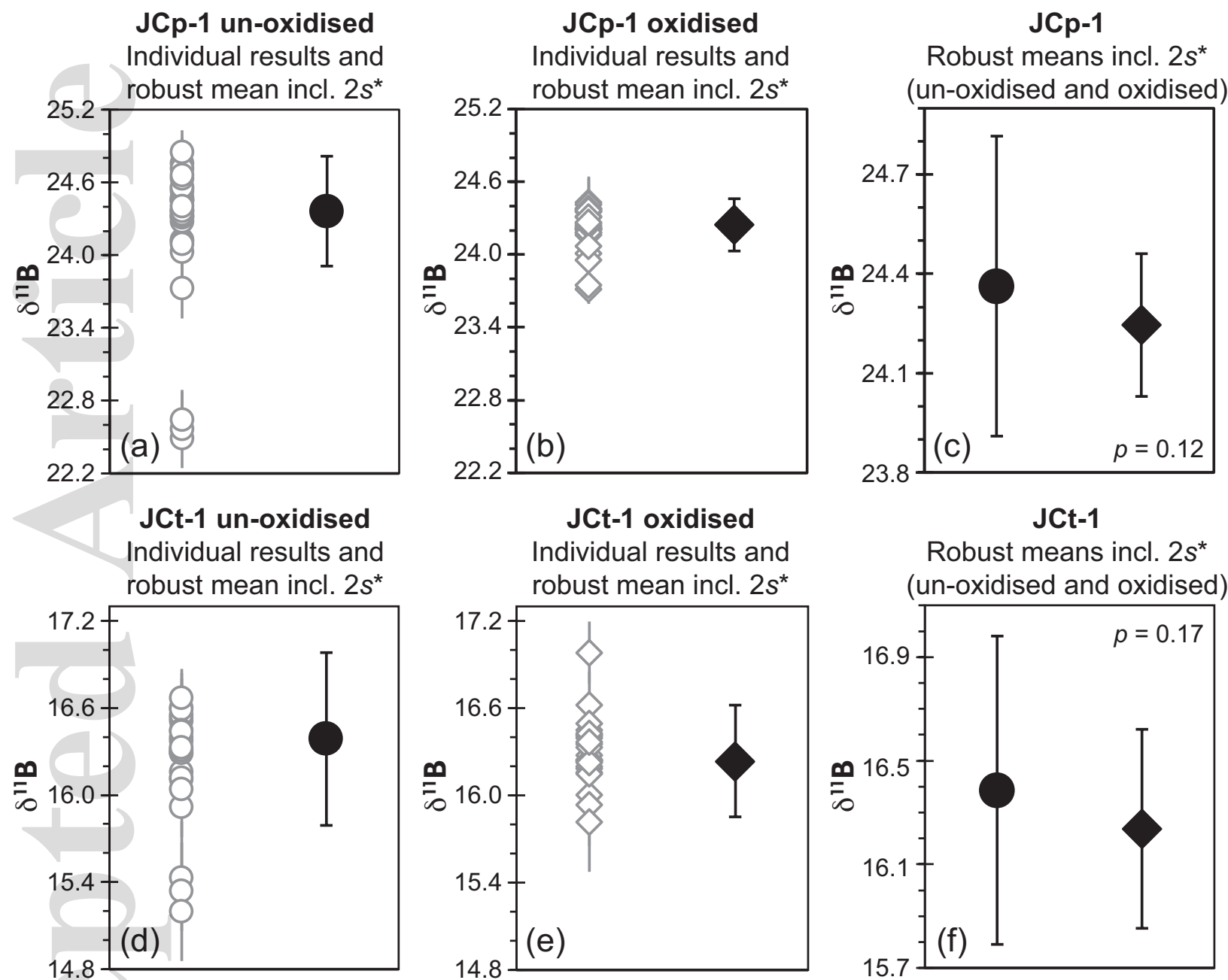




ggr_12364_f2.eps



ggr_12364_f3.eps



ggr_12364_f4.eps